PSFC/JA-07-5

Quasilinear theory of interchange modes in a closed field line configuration

Alexey Kouznetsov, [1]Jeffrey P. Freidberg and [2]Jay Kesner

May 2007

[1, 2]MIT Plasma Science and Fusion Center, 167 Albany Street, Cambridge, MA 02139, U.S.A.

This work was supported by the U.S. Department of Energy, Grant No. DE-FG02-91ER-54109.

Submitted for publication in the Physics of Plasma (April 2007)

Quasilinear theory of interchange modes

in a closed field line configuration

A. Kouznetsov, J.P. Freidberg and J. Kesner

Plasma Science and Fusion Center, Massachusetts Institute of Technology,

Cambridge, MA, 02139

ABSTRACT

Two important issues for any magnetic fusion configuration are the maximum achievable values of beta and energy confinement time when ideal magnetohydrodynamic (MHD) modes are excited. It is well known that the excitation of the MHD unstable modes typically can lead to violent restructuring of the plasma profiles. The particle and energy transport associated with these modes normally dominates all other transport mechanisms and can lead to plasma disruptions and a rapid loss of energy. This paper analytically investigates the transport of particle density, energy and magnetic field due to the ideal MHD interchange mode in a closed line system using the quasilinear approximation. The transport equations are derived for a static plasma in a hard core Z-pinch configuration and generalized to an arbitrary axisymmetric toroidal closed poloidal filed line configuration. It is shown that violation of the marginal stability criterion leads to rapid quasilinear transport that drives the pressure profile back to its marginal profile and forces the particle density to be inversely proportional to $\oint dl / B$. The applicability of the quasilinear approximation is numerically tested for the hard core Z-pinch magnetic configuration using a full nonlinear code.

I. Introduction

The goal of this paper is to derive a model for plasma transport in an axisymmetric closed-line poloidal field line systems when the plasma is weakly unstable to the interchange mode. The primarily experimental application of the analysis is to the Levitated Dipole Experiment (LDX) [1-2]. LDX, a joint MIT and Columbia University experiment, has a plasma confined in a poloidal field created by superconducting current ring, which is magnetically levitated in a large vacuum chamber.

There is a key difference between the LDX and tokamak approaches to stabilize a plasma against interchange modes. The tokamak approach requires an appropriately chosen magnetic shear profile. The shear stabilizes the interchange mode, which for a tokamak is an incompressible mode. LDX, on the other hand, has only a poloidal field, and stability is provided by plasma compressibility, since there is no shear (i.e. $q = 0$).

As with any magnetic configuration, it is desirable that LDX be operated in a regime that is magnetohydrodynamically (MHD) stable. The linear MHD stability of a plasma in a hard core Z-pinch (the cylindrical analog to the LDX configuration), a point dipole configuration, and the actual toroidal LDX configuration has been extensively studied by several authors [3-6]. Each of these studies show that MHD stable profiles do indeed exist at relatively high values of β. Qualitatively, stability requires a pressure profile that decreases sufficiently gradually beyond the peak pressure.

However, even though interesting stable profiles exist theoretically, the natural profiles arising from heating a plasma governed by classical transport are almost always driven into a region that is unstable to MHD interchange modes. It then becomes important to carry out a nonlinear analysis to determine whether the plasma has a "soft landing" returning to its marginal state but with enhanced transport or a "hard landing" corresponding to a disruption.

The usual approach to determine the nonlinear evolution involves large scale numerical simulations, often involving lengthy, time consuming studies since they must track the evolution of the system on the Alfven time scale. A different approach employed in this study involves the derivation of an analytical model based on the ideas of quasilinear transport. The model ultimately predicts the nonlinear energy and particle transport of the plasma in a region of weakly unstable interchange modes. The assumption of weak instabilities is motivated by the idea that heating occurs slowly compared to the ideal MHD time scale. Thus, during a normal time evolution the plasma starts off stable, becomes weakly unstable as it heats up, and because of rapid quasilinear transport, the profiles re-adjust themselves before the modes can grow to a large enough amplitude where the full nonlinear effects dominate.

To put the present results in perspective, it is useful to revisit several previous efforts aimed at studying the nonlinear dynamics of MHD unstable systems. A state of the art 3-D code that solves the multi-dimensional system of nonlinear MHD equations is NIMROD [7]. This code is actively used by tokamak community and produces valuable insights into the MHD dynamics of a plasma. As might be expected such simulations require significant computational resources. One such study for LDX required days of computing time. The results were interesting and in a qualitative sense were consistent with the present results. Even so, it was difficult to carry out a large number of studies to determine the critical scaling relations required for experimental predictions.

In general the simulation of a closed field line system is likely to be more efficient than that of a tokamak because of the simpler geometry. There are, nevertheless, several additional complications. D. Ryutov has showed that the numerical viscosity and diffusivity necessary for proper numerical conversion can lead to error accumulation which is more severe in a closed line system than a tokamak [8]. This can change the nonlinear self-consistent saturated plasma profiles. Another concern with any nonlinear simulation that requires a substantial numerical viscosity and resistivity for convergence is the preferential damping of the small-scale turbulences in favor of the global modes. This is particularly important for the interchange instability in which the fastest growing modes occur for $k_\perp \to \infty$. Finally, in order to save computing time, many nonlinear 3-D simulations start with a plasma that is either strongly unstable initially, or else is heated at a very rapid raid to quickly generate strong instabilities. This is not the typical experimental situation and almost by definition minimizes the effect of quasilinear transport.

A simpler task for numerical simulations involves the hardcore Z-pinch, which is the large aspect ratio limit of a toroidal dipole. Both magnetic configurations represent closed filed line systems with the interchange mode imposing the most restrictive MHD stability condition. The simplification arises because the hard core Z-pinch interchange mode requires a 2-D rather than a 3-D simulation. Pastukhov and Chudin modeled the system of reduced MHD equations for an unstable hard core Z-pinch plasma [9-10]. The key result was that violation of the marginal stability did not lead to a disruption, but resulted in non-local anomalous transport through the global plasma motion. A large-scale convective motion of the plasma enhanced the energy transport to balance the heating source, thus keeping the system close to marginal stability. Anomalous transport due to macroscopic convective cells was also separately reported by Makhnin *et al.* [11] and Adler and Hassam [12]. Adler and Hassam forced the convective cells by the asymmetric energy and particle sources, while Makhnin reported short-lived random convective cells that were later replaced by a chaotic turbulence.

Summarizing, the numerical codes do provide valuable insights into the dynamics of an MHD unstable system, but often require significant computational resources and have internal numerical limitations, which may affect the results. These limitations have prevented the determination of detailed scaling relations for the energy confinement time and plasma β which are of great practical importance to experiments.

An alternative approach, employed in this study, is to create an analytical model, which predicts the energy and particle transport of a plasma in the region weakly unstable to the interchange mode. It is shown that an excitation of MHD instabilities creates new type of transport, seen in quasilinear approximation. We have employed this approximation to derive transport equations in the MHD unstable region and have shown that the quasilinear transport relaxes the system back to marginal stability.

The present approach involves the derivation of a set of quasilinear transport equations where the perturbations are driven by the ideal MHD interchange instability. The analysis is carried out for both the hard core Z-pinch and toroidal dipole geometries. We show that while the quasilinear transport coefficients depend on the saturated amplitudes of the perturbations, it is not necessary in practice to explicitly calculate these amplitudes in order to deduce the values of τ_E and β. The key results of the analysis are as follows. First, we prove the often made conjecture that the plasma pressure will relax to its marginal profile. Second, the quasilinear theory makes a specific prediction concerning the density profile - $n \sim \left(\oint dl/B\right)^{-1}$. This allows us to predict the peak temperature. Third, specific scaling relations are derived for τ_E and β in the accompanying paper.

The paper is organized as follows: Section 2 discusses the basics issues of the quasilinear approach. In Section 3 the full quasilinear transport equations are derived for the hard core Z-pinch geometry. Section 4 presents the derivation of the steady state transport model for the hard core Z-pinch. The full quasilinear transport equations are rewritten in a more transparent form which can then be reduced using the assumption that quasilinear transport is the dominant transport mechanism. A simple model is used to illustrate the validity of the approximations. In Section 5, the quasilinear transport equations are generalized to a toroidal axisymmetric closed-field line magnetic configuration. Finally, Section 6 presents non-linear numerical simulations of the evolution of an unstable plasma in a hard-core Z-pinch configuration. We test the applicability of the ideal MHD quasilinear model derived earlier and discuss the implications for predicting plasma profiles.

II. MHD quasilinear transport – basic issues

In this section we discuss the basic issues arising in the formulation of MHD quasilinear transport arising from ideal MHD interchange modes in an axisymmetric, closed line, toroidal configuration. This configuration includes the levitated dipole configuration as well as its large aspect ratio limit, the hard core Z-pinch.

For the system under consideration the primary unknowns to be determined are the pressure p, density ρ, poloidal magnetic field $\mathbf{B}_p$, and the diffusion velocity $\mathbf{v}$. Following the standard procedures used in the quasilinear theory of kinetic instabilities [13] we expand all unknowns as

$$Q(\mathbf{r},t) = \bar{Q}(\psi,\varepsilon t) + \tilde{Q}(\psi,\chi,\phi,t) \tag{1}$$

Note that we have introduced flux coordinates where the "radial" coordinate ψ is tied to the background magnetic field, χ is an arbitrary poloidal angle, and ϕ is the standard toroidal angle. The various quantities $\bar{Q}(\psi,\varepsilon t)$ represent the background state of the plasma. These are one-dimensional functions which are allowed to vary slowly with time due to the quasilinear plus classical evolution of the system. It is the evolution of the $\bar{Q}(\psi,\varepsilon t)$ with respect to the background flux that is the primary goal of the analysis.

The quantities $\tilde{Q}(\mathbf{r},t)$ represent the perturbations away from equilibrium due to MHD instabilities and are responsible for driving the quasilinear transport. Their amplitudes are assumed to be small enough (e.g. $\tilde{Q} \ll \bar{Q}$) so that nonlinear effects can be neglected, but still large enough that the resulting quasilinear diffusion dominates classical transport. Mathematically, the perturbed quantities represent a sum over the unstable linear eigenmodes of the system with each mode calculated by neglecting the slow variation of the background state. In the analysis the perturbations are assumed to arise solely from interchange instabilities.

Collisional effects, such as resistivity and thermal conductivity also lead to transport of energy and particles as well as affecting the growth rates and eigenmodes of the MHD perturbations. These effects are considered in detail Section V. Qualitatively, these effects are important in regions of the pressure profile where localized interchange modes are stable. In these regions collisional effects then represent the only source of transport. In the unstable regions, the ideal MHD modes typically have a much faster time scale than any collisional transport contributions. Therefore, we assume that collisional effects do not significantly alter the growth rates or change the eigenfunctions of the unstable perturbations.

An important conclusion from the analysis, applicable in the interesting regime where the quasilinear transport coefficients are much larger than those due to classical transport, is the following: The final steady state profiles can be uniquely determined and are independent of the value of the quasilinear transport coefficients. There is no need to explicitly calculate the saturated amplitudes of the unstable MHD modes.

With this as background we are now ready to begin the detailed analysis of quasilinear transport in the MHD model.

III. Quasilinear transport in a hard core Z-pinch

The first geometry of interest is the hard core Z-pinch, a cylindrically symmetric configuration for which the analysis is highly simplified. The analysis separates into two contributions, one from the MHD stable region that is assumed to obey the laws of classical transport, the other from the region that is unstable to MHD interchange modes.

A general 1-D transport equation is derived that is valid in both regions, followed by a simple calculation that shows how the two regions can be separated and then connected across the marginal stability boundary.

- **The general 1-D transport equations**

It is well known [14] that a hard-core Z-pinch is potentially unstable to only two ideal MHD modes: the $m = 0$ interchange mode and the $m = 1$ helical mode. Here, m is the azimuthal wave number. The interchange mode imposes the strictest limitations on the plasma profile and sets the value of the maximum achievable local pressure gradient. The fastest growing interchange modes are localized in space and occur for large longitudinal wave numbers (i.e. $k \to \infty$). For the LDX configuration the outer portion of the profile, beyond the location of the pressure peak, is the region likely to be unstable to interchange modes. See Fig.1. The inner region, where the pressure gradient is positive, is stable to interchange modes. It is in this region that classical transport is assumed. Our goal here is to derive a set of 1-D transport equations valid in both regions.

The starting point for the analysis is a simplified, nonlinear single fluid model that includes thermal conductivity, resistivity, and the thermal force, but for simplicity neglects viscosity. The starting model is thus given by

$$
\begin{aligned}
&\frac{\partial n}{\partial t} + \nabla \cdot (n\,\mathbf{v}) = 0 \\
&m_i n\left(\frac{\partial \mathbf{v}}{\partial t} + \mathbf{v}\cdot\nabla\mathbf{v}\right) = \mathbf{J}\times\mathbf{B} - \nabla p \\
&\frac{d}{dt}\left(\frac{p}{n^\gamma}\right) = \frac{\gamma-1}{n^\gamma}\left[\nabla\cdot\left(n\vec{\vec{\chi}}\cdot\nabla T\right) + S\right] \\
&\frac{\partial \mathbf{B}}{\partial t} = \nabla\times\left[\mathbf{v}\times\mathbf{B} - \eta\left(\mathbf{J} - \frac{3}{2}\frac{n\,\mathbf{B}\times\nabla T}{B^2}\right)\right]
\end{aligned} \tag{2}
$$

Here $S(\mathbf{r},\varepsilon t)$ is the heating source. Note that we have included the thermal force in Ohm's law in order to prevent the simple, but physically unrealistic result that the pressure in the MHD stable region is driven to be uniform in space; that is, the pressure would be unconfined if the thermal force is neglected. Also, although the thermal diffusivity is written as a tensor, the analysis shows that only the cross-field component enters into the analysis.

The model is reduced as follows. The background quantities $\bar{\rho}(r,\varepsilon t)$, $\bar{p}(r,\varepsilon t)$, $\bar{B}_\theta(r,\varepsilon t)$, and $\bar{v}_r(r,\varepsilon t)$ are the primary unknowns to be determined. For simplicity, we assume that the velocity of the background state of the plasma is due solely to transport. (i.e. there is no large background flow velocity). This implies that we can neglect inertial effects in the momentum equation for the background state.

Consider next the perturbations. For $m = 0$ interchange modes, the perturbations are, by definition, functions only of (r,z,t). Also, the perturbed magnetic field has only a parallel component: $\tilde{\mathbf{B}} = \tilde{B}_\theta(r,z,t)\mathbf{e}_\theta$. In contrast, the perturbed velocity has no parallel component: $\tilde{\mathbf{v}} = \tilde{v}_r(r,z,t)\,\mathbf{e}_r + \tilde{v}_z(r,z,t)\,\mathbf{e}_z$. All perturbed quantities are assumed to be a sum over unstable interchange eigenfunctions:

$$
\tilde{Q}(r,z,t) = \sum_n Q_n(r)\exp(-i\omega_n t + ik_n z) \tag{3}
$$

where $k = n / R_0$ and R_0 is the major radius of the equivalent torus.

Under the above assumptions the starting equations reduce to

$$\begin{aligned}
&\frac{\partial n}{\partial t} + \nabla \cdot (n\mathbf{v}) = 0 \\
&\frac{\partial s}{\partial t} + \nabla \cdot (s\mathbf{v}) = \frac{\gamma - 1}{n^{\gamma-1}}\left[\nabla \cdot (n\tilde{\boldsymbol{\chi}} \cdot \nabla T) + S\right] \\
&\frac{\partial}{\partial t}\left(\frac{B_\theta}{r}\right) + \nabla \cdot \left(\frac{B_\theta}{r}\mathbf{v}\right) = \nabla \cdot \left[\frac{\eta}{\mu_0 r^2}\nabla(rB_\theta) + \frac{3}{2}\frac{\eta n}{rB_\theta}\nabla T\right] \\
&m_i n\left(\frac{\partial \mathbf{v}}{\partial t} + \mathbf{v} \cdot \nabla \mathbf{v}\right) = -\nabla\left(p + \frac{B_\theta^2}{2\mu_0}\right) - \frac{B_\theta^2}{\mu_0 r}
\end{aligned} \tag{4}$$

Here, $s = p / n^{\gamma-1}$ is a function related to the entropy per unit volume and ∇ represents the two dimensional operator $\nabla = \mathbf{e}_r \partial / \partial r + \mathbf{e}_z \partial / \partial z$.

- **The magnetic field equation**

To proceed we focus on the magnetic field equation. The various quantities are substituted and after a short calculation we obtain the unexpanded but cumbersome equation given by

$$\begin{aligned}
&\frac{\partial}{\partial t}\left(\bar{B}_\theta + \tilde{B}_\theta\right) + \frac{\partial}{\partial r}\left(\bar{B}_\theta \bar{v}_r + \bar{B}_\theta \tilde{v}_r + \tilde{B}_\theta \bar{v}_r + \tilde{B}_\theta \tilde{v}_r\right) + \frac{\partial}{\partial z}\left(\bar{B}_\theta \tilde{v}_z + \tilde{B}_\theta \tilde{v}_z\right) \\
&\qquad = \frac{\partial}{\partial r}\left[\frac{\eta}{\mu_0 r}\frac{\partial}{\partial r}\left(r\bar{B}_\theta\right) + \frac{3}{2}\frac{\eta \bar{n}}{\bar{B}_\theta}\frac{\partial \bar{T}}{\partial r}\right]
\end{aligned} \tag{5}$$

Note that both background and perturbation contributions have been included on the left hand side of the equation. However, the perturbations have been neglected on the right hand side since the classical transport terms are already assumed to be small compared to the MHD terms.

The next step is to average the equation over z to obtain the governing equation for the background magnetic field. The averaging procedure is defined as

$$\langle Q\rangle = \frac{1}{2\pi L}\int_0^{2\pi L} Q\, dz \tag{6}$$

where $L = 2\pi / k_1$ is the longest wavelength of the unstable perturbations and by definition $\langle \tilde{Q}\rangle = 0$. After averaging, Eq. (5) reduces to

$$\frac{\partial \bar{B}_\theta}{\partial t} + \frac{\partial}{\partial r}\left(\bar{B}_\theta \bar{v}_r\right) = -\frac{\partial}{\partial r}\left[\left\langle \tilde{B}_\theta \tilde{v}_r\right\rangle + \frac{2\eta \bar{T}^{3/4}}{\bar{B}_\theta}\frac{\partial}{\partial r}\left(\bar{n}\bar{T}^{1/4}\right)\right] \tag{7}$$

In deriving Eq. (7) we have used the background pressure balance relation

$$\frac{\partial \bar{p}}{\partial r} + \frac{\bar{B}_\theta}{\mu_0 r}\frac{\partial}{\partial r}\left(r\bar{B}_\theta\right) = 0 \tag{8}$$

obtained by averaging the momentum equation and neglecting inertial effects for the slowly evolving background state. Observe that the first term on the right hand side represents quasilinear transport while the second term corresponds to classical transport.

Equation (7) can be further simplified by introducing the background flux function $\bar{\psi}\left(r, \varepsilon t\right)$ as follows

$$\bar{B}_\theta = \frac{\partial \bar{\psi}}{\partial r} \tag{9}$$

This allows us to integrate the equation yielding

$$\frac{\partial \bar{\psi}}{\partial t} + \bar{v}_r \frac{\partial \bar{\psi}}{\partial r} = -\left\langle \tilde{B}_\theta \tilde{v}_r\right\rangle - \frac{2\eta \bar{T}^{3/4}}{\bar{B}_\theta}\frac{\partial}{\partial r}\left(\bar{n}\bar{T}^{1/4}\right) \tag{10}$$

Here, the free integration function has been set to zero under the assumption that there is no external E_z field driving the toroidal current.

- **Flux coordinates**

Equation (10) describes the evolution of the magnetic flux. It is useful because it allows us to introduce flux coordinates that define the reference frame with respect to which transport can be measured. The flux surface transformation is defined by

$$\begin{aligned} \overline{\psi} &= \overline{\psi}(r,t) \\ \tau &= t \end{aligned} \tag{11}$$

The critical relations required to carry out the analysis are easily calculated and are given by

$$\begin{aligned} \frac{\partial}{\partial r} &= \overline{B}_\theta \frac{\partial}{\partial \overline{\psi}} & \frac{\partial}{\partial t} &= \frac{\partial}{\partial \tau} - \overline{B}_\theta r_\tau \frac{\partial}{\partial \overline{\psi}} \\ r_{\overline{\psi}} &= \frac{1}{\overline{B}_\theta} & r_\tau &= -\frac{\overline{\psi}_t}{\overline{B}_\theta} \end{aligned} \tag{12}$$

When the coordinate transformation is substituted into the flux evolution equation, the result is an explicit expression for the diffusion velocity measured with respect to the reference coordinate system.

$$\overline{v}_r - r_\tau = -\frac{\left\langle \tilde{B}_\theta \tilde{v}_r \right\rangle}{\overline{B}_\theta} - \frac{2\eta \overline{T}^{3/4}}{\overline{B}_\theta} \frac{\partial}{\partial \overline{\psi}} \left(\overline{n} \overline{T}^{1/4} \right) \tag{13}$$

This equation contains the essential information required to determine the transport evolution of the plasma particles and energy.

- **Particle and energy transport**

The particle and energy transport equations are determined in a manner completely analogous to the derivation of the magnetic field equation. The expansions are substituted into the nonlinear equations which are then averaged over z. The resulting equations are further simplified by eliminating the radial velocity by means of Eq. (13). After a straightforward but slightly lengthy calculation we obtain the following evolution equations for $\bar{n}$ and $\bar{s}$.

$$\begin{aligned}
&\frac{\partial}{\partial\tau}\left(\frac{r\bar{n}}{\bar{B}_\theta}\right) = -\frac{\partial}{\partial\bar{\psi}}\left\{r\left[\langle\tilde{n}\,\tilde{v}_r\rangle - \frac{\bar{n}}{\bar{B}_\theta}\langle\tilde{B}_\theta\tilde{v}_r\rangle - D_C\bar{B}_\theta\left(\frac{\partial\bar{n}}{\partial\bar{\psi}} + \frac{\bar{n}}{4\bar{T}}\frac{\partial\bar{T}}{\partial\bar{\psi}}\right)\right]\right\} \\
&\frac{\partial}{\partial\tau}\left(\frac{r\bar{s}}{\bar{B}_\theta}\right) = -\frac{\partial}{\partial\bar{\psi}}\left\{r\left[\langle\tilde{s}\,\tilde{v}_r\rangle - \frac{\bar{s}}{\bar{B}_\theta}\langle\tilde{B}_\theta\tilde{v}_r\rangle - \frac{D_C\bar{B}_\theta\bar{s}}{n}\left(\frac{\partial\bar{n}}{\partial\bar{\psi}} + \frac{\bar{n}}{4\bar{T}}\frac{\partial\bar{T}}{\partial\bar{\psi}}\right)\right]\right\} \\
&\qquad\qquad + \frac{\gamma-1}{\bar{n}^{\gamma-1}}\left[\frac{\partial}{\partial\bar{\psi}}\left(r\bar{n}\bar{B}_\theta\chi_C\frac{\partial\bar{T}}{\partial\bar{\psi}}\right) + \frac{r\langle S\rangle}{\bar{B}_\theta}\right]
\end{aligned} \tag{14}$$

Here, $D_C = 2\eta\bar{n}\bar{T}/\bar{B}_\theta^2 \sim \rho_e^2/\tau_{ei}$ and $\chi_C = 2\bar{T}/m_i\omega_{ci}^2\tau_{ii} \sim \rho_i^2/\tau_{ii}$.

The final step in the derivation is to substitute for the perturbed quantities in order to obtain the quasilinear transport coefficients. This is easily accomplished by noting that the equations for the perturbed quantities are obtained by subtracting the z averaged equations from the exact nonlinear equations. As in the standard quasilinear procedure the nonlinear terms are neglected in the equations for the perturbed equations. Furthermore, as stated previously, the time scale for MHD instabilities is much faster than for classical transport. The implication is that it is a good approximation to neglect the classical transport terms in the perturbation equations. The net result of these considerations is that the perturbations satisfy the equations of ideal MHD. Specifically from the conservation of mass and the conservation of flux we obtain

$$
\begin{aligned}
\tilde{n} &= -\xi \frac{\partial \bar{n}}{\partial r} - \bar{n}\nabla\cdot\boldsymbol{\xi} \\
\frac{\tilde{B}_\theta}{r} &= -\xi \frac{\partial}{\partial r}\left(\frac{\tilde{B}_\theta}{r}\right) - \frac{\tilde{B}_\theta}{r}\nabla\cdot\boldsymbol{\xi}
\end{aligned}
\tag{15}
$$

where $\tilde{\mathbf{v}} \approx -i\omega\boldsymbol{\xi} = -i\omega\left(\xi\mathbf{e}_r + \xi_z\mathbf{e}_z\right)$.

From these expressions it follows that

$$
\begin{aligned}
\left\langle \tilde{n}\,\tilde{v}_r \right\rangle - \frac{\bar{n}}{\bar{B}_\theta}\left\langle \tilde{B}_\theta \tilde{v}_r \right\rangle &= -D_Q \frac{\bar{B}_\theta^2}{r}\frac{\partial}{\partial\bar{\psi}}\left(\frac{r\bar{n}}{\bar{B}_\theta}\right) \\
\left\langle \tilde{s}\,\tilde{v}_r \right\rangle - \frac{\bar{s}}{\bar{B}_\theta}\left\langle \tilde{B}_\theta \tilde{v}_r \right\rangle &= -D_Q \frac{\bar{B}_\theta^2}{r}\frac{\partial}{\partial\bar{\psi}}\left(\frac{r\bar{s}}{\bar{B}_\theta}\right)
\end{aligned}
\tag{16}
$$

where D_Q is the quasilinear diffusion coefficient given by

$$
D_Q\left(\bar{\psi},\tau\right) = \sum_n \gamma_n \left|\xi_n\right|^2 \tag{17}
$$

The final transport equations are obtained by substitution of Eq. (16) into Eq. (14). Also, since $D_C \sim \left(m_e/m_i\right)^{1/2}\chi_C$, it is a good approximation to neglect the D_C terms in the energy equations. This leads to

$$
\begin{aligned}
\frac{\partial}{\partial\tau}\left(\frac{rn}{B_\theta}\right) &= \frac{\partial}{\partial\psi}\left[D_Q B_\theta^2 \frac{\partial}{\partial\psi}\left(\frac{rn}{B_\theta}\right) + rD_C B_\theta\left(\frac{\partial n}{\partial\psi} + \frac{n}{4T}\frac{\partial T}{\partial\psi}\right)\right] \\
\frac{\partial}{\partial\tau}\left(\frac{rs}{B_\theta}\right) &= \frac{\partial}{\partial\psi}\left[D_Q B_\theta^2 \frac{\partial}{\partial\psi}\left(\frac{rs}{B_\theta}\right)\right] + \frac{\gamma-1}{n^{\gamma-1}}\left[\frac{\partial}{\partial\psi}\left(r\chi_C n B_\theta \frac{\partial T}{\partial\psi}\right) + \frac{r\left\langle S\right\rangle}{B_\theta}\right]
\end{aligned}
\tag{18}
$$

where for simplicity of notation the over-bars have been suppressed on the background variables. These are the desired quasilinear transport equations. The basic unknowns are $p(\psi,\tau), n(\psi,\tau),$ and $r(\psi,\tau)$. The relationships to the variables appearing in Eq. (18) are as follows: $p = n^{\gamma-1}s$, $T = n^{\gamma-2}s/2$, and $B_\theta = 1/r_\psi$. One more equation is needed to close the system and this is the pressure balance relation for the background state. This equation determines $r(\psi)$ and in flux coordinates reduces to

$$\frac{\partial^2 r}{\partial \psi^2} = \frac{1}{r}\left(\frac{\partial r}{\partial \psi}\right)^2 + \frac{\partial p}{\partial \psi}\left(\frac{\partial r}{\partial \psi}\right)^3 \tag{19}$$

The derivation of the 1-D quasilinear transport equations is now complete.

IV. One dimensional steady state transport

- **Reduction of the equations**

One practical application of the quasilinear transport equations is to determine the steady state profiles of a hard core Z-pinch in which one portion of the profile is stable to interchange modes while another is unstable. The formulation of multi-region problem is carried out in this Section. It is also shown, by means of a model problem, how the formulation can be substantially simplified in the interesting regime where $D_Q \gg \chi_C$. Interestingly, the final results are closely coupled to the results of linear MHD stability although in the derivation of the quasilinear transport equations described above only the linearized mass and magnetic field equations have been used – no use has been made of the linearized momentum equation.

In steady state (i.e. $\partial / \partial \tau = 0$) the quasilinear equations can be simplified by reverting back to radial rather than flux coordinates since there is a one-to-one relation between ψ and r: $\psi(r,t) \to \psi(r)$. The steady state equations are thus given by

$$
\begin{aligned}
&\frac{\partial}{\partial r}\left[D_Q B_\theta \frac{\partial}{\partial r}\left(\frac{rn}{B_\theta}\right)+rD_C\left(\frac{\partial n}{\partial r}+\frac{n}{4T}\frac{\partial T}{\partial r}\right)\right]=0\\
&\frac{\partial}{\partial r}\left[D_Q B_\theta \frac{\partial}{\partial r}\left(\frac{rs}{B_\theta}\right)\right]+\frac{\gamma-1}{n^{\gamma-1}}\left[\frac{\partial}{\partial r}\left(r\chi_C n\frac{\partial T}{\partial r}\right)+r\langle S\rangle\right]=0
\end{aligned}
\tag{20}
$$

Equation (20) can be written in a slightly different form that more closely shows the connection between the quasilinear transport terms and MHD interchange stability. By making use of the background radial pressure balance relation it can be shown that Eq. (20) can be rewritten as

$$
\begin{aligned}
&\frac{\partial}{\partial r}\left[D_Q n\left(K_n+\frac{\mu_0 p}{B_\theta^2}K_p\right)+rD_C\left(\frac{\partial n}{\partial r}+\frac{n}{4T}\frac{\partial T}{\partial r}\right)\right]=0\\
&\frac{\partial}{\partial r}\left\{D_Q\frac{p}{n^{\gamma-1}}\left[\left(1+\frac{\mu_0 p}{B_\theta^2}\right)K_p-(\gamma-1)K_n\right]\right\}+\frac{\gamma-1}{n^{\gamma-1}}\left[\frac{\partial}{\partial r}\left(r\chi_C n\frac{\partial T}{\partial r}\right)+r\langle S\rangle\right]=0
\end{aligned}
\tag{21}
$$

where

$$
\begin{aligned}
K_p(r)&=\frac{r}{p}\frac{dp}{dr}+\frac{2\gamma B_\theta^2}{B_\theta^2+\mu_0\gamma p}\\
K_n(r)&=\frac{r}{n}\frac{dn}{dr}+\frac{2B_\theta^2}{B_\theta^2+\mu_0\gamma p}
\end{aligned}
\tag{22}
$$

Observe that the condition for stability against localized interchange modes, as first derived by Kadomstev [14], is given by $K_p(r)>0$. Intuitively we see that in the limit of quasilinear diffusion dominance (i.e. $D_Q/D_C\rightarrow\infty$) the plasma profiles must relax to a state corresponding to $K_p\rightarrow 0$ and $K_n\rightarrow 0$. In other words, the profiles relax so as to just hover around the point of marginal stability.

It is also worth emphasizing that D_Q is large only in regions that are unstable to interchange modes. For a hard core Z-pinch only the outer portion of the pressure profile is potentially unstable. The implication is that to take this stable-unstable transition into account D_Q must be of the form

$$D_Q = D_Q(r)H(-K_p) \tag{23}$$

where H is the Heaviside step function.

Consider next the solution to the steady state transport equations for large but finite D_Q. In principle, we must solve the equations separately in the stable and unstable regions and then match the density and temperature plus the particle flux and energy flux across the critical radius corresponding to marginal stability. We show below, by means of a model problem, that for large D_Q, the solutions and the matching procedure are greatly simplified if our main goal is to calculate certain average quantities such as the plasma β or the energy confinement time τ_E.

- **Model problem**

A model problem that captures the essential physics of the quasilinear transport analysis is as follows

$$\frac{1}{r}\frac{d}{dr}\left[rD_C\frac{dp}{dr} + rD_Q\left(\frac{dp}{dr} + \frac{2p}{r}\right)\right] + S = 0 \tag{24}$$

subject to boundary conditions $p'(0) = 0,\ p(1) = p_w$. For simplicity we assume that $D_C, D_Q,$ and S are constants. The condition to excite an MHD instability, in analogy with the quasilinear model, is taken to be

$$\frac{dp}{dr} + \frac{2p}{r} \le 0 \tag{25}$$

As a reference case we can easily calculate the solution for purely classical transport (i.e. $D_Q = 0$ everywhere). The solution is given by

$$p = p_0\left(1 + \varepsilon - r^2\right) \tag{26}$$

where $p_0 = S/4D_C$ and $\varepsilon = p_w / p_0$. The heating power is assumed to be sufficiently large so that the edge pressure is much less than the central pressure: $p_w / p_0 = \varepsilon \ll 1$.

It can easily be shown that the classical solution would be MHD unstable in the region $r_s^2 < r^2 < 1$ where $r_s^2 = (1+\varepsilon)/2 \approx 1/2$. Lastly, our end goal is to calculate the volume averaged pressure defined by

$$\langle p \rangle = 2\int_0^1 p\, r dr \tag{27}$$

A short calculation shows that for the case of classical transport

$$\langle p \rangle = \frac{p_0(1+2\varepsilon)}{2} \approx \frac{p_0}{2} \tag{28}$$

Consider now the model problem including quasilinear transport. We obtain the desired solutions by solving in the inner stable region $0 < r^2 < r_s^2$ using only classical transport (i.e. $D_Q = 0$). In the unstable region $r_s^2 < r^2 < 1$ we use the full equation with $D_Q \ne 0$. Note that at this point the marginally stable transition point r_s^2 is still an unknown quantity to be determined.

The solutions in each region are easily obtained and can be written as

$$
\begin{array}{lll}
\text{Classical:} & p = p_0\left(c_1 - r^2\right) & 0 < r^2 < r_s^2 \\
\text{Quasilinear:} & p = p_0\left(c_2 + \dfrac{c_3}{r^{2\alpha}} - \dfrac{\delta}{1+\delta} r^2\right) & r_s^2 < r^2 < 1
\end{array}
\tag{29}
$$

Here, the c_j are free integration constants, $\delta = D_C / 2D_Q \ll 1$, and $\alpha = 1/(1+2\delta)$.

The problem as it now stands has four unknown constants: c_1, c_2, c_3, and r_s^2. These are determined by the following four conditions: (1) the wall condition $p(1) = p_w$, (2) the requirement that the classical solution be marginally stable at $r = r_s^-$, which is equivalent to $\left[p' + 2p/r\right]_{r=r_s^-} = 0$, (3) continuity of the pressure across the marginal stability transition point $[\![p]\!]_{r=r} = 0$, and (4) continuity of the flux across the marginal stability transition point $[\![p']\!]_{r=r_s} = 0$. Note that the last condition is simplified because r_s corresponds to the point of marginal stability as dictated by condition (2). After a short calculation the unknown constants can be determined and substituted back into Eq. (29), yielding

$$
\begin{array}{lll}
\text{Classical:} & p = p_0\left(2r_s^2 - r^2\right) & 0 < r^2 < r_s^2 \\
\text{Quasilinear:} & p = p_0\left(\dfrac{1+2\delta}{1+\delta}\dfrac{r_s^{2+2\alpha}}{r^{2\alpha}} - \dfrac{\delta}{1+\delta} r^2\right) & r_s^2 < r^2 < 1
\end{array}
\tag{30}
$$

where

$$
r_s^2 = \left[\frac{\varepsilon(1+\delta)+\delta}{1+2\delta}\right]^{\frac{1}{1+\alpha}} \tag{31}
$$

The final quantity of interest is the average pressure which, when evaluated, has the following somewhat complex form

$$
\langle p \rangle = p_0\left[\frac{(1+2\delta)^2}{2\delta(1+\delta)}\left(r_s^{2+2\alpha} - r_s^4\right) - \frac{\delta}{1+\delta}\frac{1-r_s^4}{2}\right] \tag{32}
$$

In the interesting physical limit of large quasilinear diffusion, corresponding to $\delta \ll \varepsilon \ll 1$, the expressions become independent of δ and simplify to

$$
\begin{aligned}
& r_s^2 \approx \varepsilon^{1/2} \\
& \langle p \rangle \approx \frac{p_0}{2}\left(3\varepsilon - \varepsilon \ln \varepsilon\right)
\end{aligned}
\tag{33}
$$

The key point of the model problem is to show how Eq. (33) can be obtained by a much simpler procedure by taking the small δ limit at the beginning, rather than the end of the calculation. The simpler procedure consists of solving the classical transport equations for the inner part of the profile and using the marginal stability condition to determine the pressure in the outer part of the profiles. Specifically, we need to solve

$$
\begin{aligned}
& \frac{1}{r}\frac{d}{dr}\left(rD_C\frac{dp}{dr}\right) + S = 0 \qquad && 0 < r^2 < r_s^2 \\
& \frac{dp}{dr} + \frac{2p}{r} = 0 && r_s^2 < r^2 < 1
\end{aligned}
\tag{34}
$$

The boundary conditions are (1) $p'(0) = 0$ and (2) $p(1) = p_w$. The marginal stability point is again determined by requiring that the classical solution satisfy $\left[p' + 2p/r\right]_{r=r_s^-} = 0$. The main simplification that occurs involves the jump conditions. In this case only one jump condition is required $[\![p]\!]_{r=r_s} = 0$. The problem is now completely specified. The solution is found to be

$$
\begin{aligned}
& p = p_0(2\varepsilon^{1/2} - r^2) \qquad && 0 < r^2 < \varepsilon^{1/2} \\
& p = p_0\varepsilon / r^2 && \varepsilon^{1/2} < r^2 < 1 \\
& \langle p \rangle = \frac{p_0}{2}\left(3\varepsilon - \varepsilon \ln \varepsilon\right)
\end{aligned}
\tag{35}
$$

We see that the simplified calculation leads to the same value of $\langle p \rangle$ as that obtained from the small δ limit of the full quasilinear solution. A comparison of the radial profiles corresponding to classical transport, the full quasilinear transport, and the simplified quasilinear transport are illustrated in Fig.2 for the case $\varepsilon = 10^{-2}$ and $\delta = 10^{-4}$. Observe the similarity between the simple and full quasilinear profiles and the large reduction in peak pressure with respect to the classical profiles.

- **Final form of the cylindrical quasilinear transport equations**

Based on the results from the model problem we can now simplify the formulation for the cylindrical quasilinear analysis. A key result is that in the limit of large quasilinear diffusion the final results are independent of the value of D_Q. There is no need to evaluate the nonlinear saturated amplitudes. The model simplifies as follows.

Classical region:

$$\begin{aligned}
&\frac{\partial}{\partial r}\left[rD_C\left(\frac{\partial n}{\partial r}+\frac{n}{4T}\frac{\partial T}{\partial r}\right)\right]=0 \qquad && \frac{\partial n(r_c)}{\partial r}=0\\
&\frac{\partial}{\partial r}\left(r\chi_C n\frac{\partial T}{\partial r}\right)+r\langle S\rangle=0 && T(r_c)=0
\end{aligned} \tag{36}$$

Quasilinear region:

$$\begin{aligned}
&K_p(r)=\frac{r}{p}\frac{dp}{dr}+\frac{2\gamma B_\theta^2}{B_\theta^2+\mu_0\gamma p}=0 \qquad && p(r_w)=p_w\\
&K_n(r)=\frac{r}{n}\frac{dn}{dr}+\frac{2B_\theta^2}{B_\theta^2+\mu_0\gamma p}=0 && n(r_w)=n_w
\end{aligned} \tag{37}$$

Here, r_c is the coil radius and r_w is the wall radius. The boundary conditions on the coil correspond to a perfect heat sink and 100% recycling of particles. On the wall we assume the temperature and density are specified. The formulation of the problem is completed by (1) requiring that the classical solutions satisfy the marginal stability criterion at $r = r_s^-$, corresponding to $, K_p(r_s^-) = 0$ and (2) matching the solutions across the stability interface which requires $[\![n]\!]_{r=r_s} = 0$ and $[\![p]\!]_{r=r_s} = 0$.

Once the solutions are obtained it is then a straightforward task to evaluate critical experimental parameters such as the average β and the energy confinement time τ_E. This calculation is carried out in detail in the accompanying paper.

V. Quasilinear transport in a toroidal dipole configuration

The analysis of quasilinear transport in a cylinder can be generalized to the toroidal case in a relatively straightforward manner. In a torus two additional features must be taken into account in the analysis, but these are not overly difficult tasks. First, the equilibrium geometry becomes two dimensional because of coupling to the poloidal angle. This difficulty is resolved by introducing flux coordinates. Second, because of the poloidal coupling the definition of an interchange mode is not as transparent as in a cylinder. To address this issue we focus attention on the fastest growing modes, corresponding to $n \to \infty$ where n is the toroidal mode number. These are the interchange modes and in this limit the definition becomes unambiguous.

For mathematical simplicity the analysis is carried out by taking the large D_Q limit at the outset. There are three steps in the procedure: (1) introduce flux coordinates, (2) derive the transport equations in the classical region, and (3) derive the transport equations in the quasilinear region.

- **Flux coordinates**

For a closed line axisymmetric toroidal configuration it is convenient to carry out the analysis in terms of flux coordinates defined by (1) a "radial" coordinate $\psi(R,Z)$ corresponding to the flux, (2) a "poloidal" coordinate $l(R,Z)$ corresponding to arc length, and (3) a "toroidal" coordinate ζ corresponding to the usual polar angle. The coordinates are tied to the slowly varying, background magnetic flux. Clearly, by construction, the coordinates are orthogonal. Also, in the flux coordinate system time is denoted by τ. Thus the coordinate transformation is given by

$$\begin{aligned} \psi &= \psi(R,Z,t) \\ l &= l(R,Z,t) \\ \zeta &= -\phi \\ \tau &= t \end{aligned} \tag{38}$$

Note that (ψ, l, ζ) is a right-handed system. Next, the flux is defined by again neglecting inertial effects in the momentum equation for the background quantities. The implication is that ψ satisfies the Grad-Shafranov equation

$$R^2 \nabla \cdot \left(\frac{\nabla \psi}{R^2} \right) = -\mu_0 R^2 \frac{\partial p(\psi,t)}{\partial \psi} \tag{39}$$

The magnetic field is related to the flux by the relation

$$\mathbf{B} = \frac{1}{R} \nabla \psi \times \mathbf{e}_\phi \tag{40}$$

The poloidal coordinate is chosen to be arc length, defined as

$$\mathbf{B} \cdot \nabla l = B \tag{41}$$

Three useful relations for the analysis resulting from these definitions are given by

$$R\,dR\,dZ\,d\phi = \frac{d\psi\,dl\,d\zeta}{B}$$
$$\nabla\cdot\mathbf{A} = B\left[\frac{\partial}{\partial\psi}\left(RA_n\right) + \frac{\partial}{\partial l}\left(\frac{A_{\|}}{B}\right)\right] + \frac{1}{R}\frac{\partial A_\zeta}{\partial\zeta} \tag{42}$$
$$\frac{\partial}{\partial t} = \frac{\partial}{\partial\tau} + \psi_t\frac{\partial}{\partial\psi} + l_t\frac{\partial}{\partial l}$$

where $A_n = (\nabla\psi\cdot\mathbf{A})/RB$ and $A_{\|} = \mathbf{b}\cdot\mathbf{A}$ with $\mathbf{b} = \mathbf{B}/B$. Lastly, we need an expression for the volume contained within a given flux surface $\mathsf{V}(\psi)$. We define $V = \left(1/2\pi\right)d\mathsf{V}/d\psi$ from which it follows that

$$\mathsf{V}(\psi) = 2\pi\int_0^{\psi} d\psi'\oint\frac{dl}{B}$$
$$V(\psi) = \oint\frac{dl}{B} \tag{43}$$

We are now ready to derive the transport equations.

- **Classical region**

In the classical region the analysis is purely two dimensional (i.e. ψ, l) since by definition no perturbations exist which would introduce ζ dependence. The derivation begins by focusing on the equation for the toroidal flux function. As for the cylindrical case we write $\mathbf{B} = \nabla\times\left[\left(\psi/R\right)\mathbf{e}_\phi\right]$ and then integrate Faradays law (Eq. 2), evaluating the $\mathbf{e}_\phi$ component from the resulting integrated expression. This yields

$$\frac{\partial\psi}{\partial t} + \mathbf{v}\cdot\nabla\psi = -\eta R^2\left(\frac{\partial p}{\partial\psi} - \frac{3n}{2}\frac{\partial T}{\partial\psi}\right) \tag{44}$$

Note that $T = T(\psi, t)$. It does not depend on l because of the large parallel thermal conductivity.

Next, we introduce flux coordinates into this relation, which yields an explicit expression for the normal component of velocity with respect to the coordinate velocity.

$$v_\psi + \frac{\psi_t}{RB} = -\frac{2\eta R T^{3/4}}{B}\frac{\partial}{\partial\psi}\left(nT^{1/4}\right) \tag{45}$$

Following the cylindrical analysis, we write the conservation of mass and energy relations in flux coordinates and then average over both ζ and l. After a slightly lengthy but nonetheless well-established procedure we obtain two evolutionary equations for the background particle density and entropy related function given by

$$\begin{aligned}\frac{\partial}{\partial\tau}(nV) &= \frac{\partial}{\partial\psi}\left(\bar{D}_C T^{3/4}\frac{\partial nT^{1/4}}{\partial\psi}\right)\\ \frac{\partial}{\partial\tau}(sV) &= \frac{\gamma-1}{n^{\gamma-1}}\frac{\partial}{\partial\psi}\left(n\bar{\chi}_C\frac{\partial T}{\partial\psi}\right)+\frac{\gamma-1}{n^{\gamma-1}}\langle S\rangle V\end{aligned} \tag{46}$$

where

$$\begin{aligned}\langle Q\rangle &= \frac{\oint Q\frac{dl}{B}}{\oint\frac{dl}{B}}\\ \bar{D}_C &= 2\eta nTV\left\langle R^2\right\rangle = V\left\langle R^2B^2D_C\right\rangle\\ \bar{\chi}_C &= V\left\langle R^2B^2\chi_C\right\rangle\end{aligned} \tag{47}$$

As for the cylindrical case we have neglected particle diffusion as compared to thermal diffusion in the entropy equation.

- **Quasilinear region**

The analysis in the quasilinear region is in general three dimensional since the unstable perturbations are of the form $\tilde{Q}(\psi,l,\zeta,\tau)=\tilde{Q}(\psi,l)\exp(-i\omega\tau+in\zeta)$. However, previous analysis of the MHD stability of closed line systems [4] has shown that the most unstable modes, in terms of thresholds, are high n interchanges. This recognition, combined with the fact that quasilinear transport drives the profiles close to marginal stability, substantially simplifies the analysis. In this limit we can introduce a small parameter $\delta=\gamma_n a/v_{Ti}\ll 1$. Here γ_n is the MHD growth rate which is small since the system hovers near marginal stability. For small δ the form of the MHD perturbations simplifies as follows.

$$\begin{aligned}
\boldsymbol{\xi}(\psi,l) &\approx \boldsymbol{\xi}_\perp(\psi,l)+\delta^2\boldsymbol{\xi}_\parallel(\psi,l)\\
\tilde{\mathbf{v}}(\psi,l) &\approx \tilde{\mathbf{v}}_\perp(\psi,l)+\delta^2\tilde{\mathbf{v}}_\parallel(\psi,l)\\
\tilde{n}(\psi,l) &\approx \tilde{n}(\psi)+\delta^2\tilde{n}_1(\psi,l)\\
\tilde{p}(\psi,l) &\approx \tilde{p}(\psi)+\delta^2\tilde{p}_1(\psi,l)\\
\tilde{\mathbf{B}}(\psi,l) &\approx \tilde{\mathbf{B}}_\parallel(\psi,l)+\delta^2\tilde{\mathbf{B}}_\perp(\psi,l)
\end{aligned} \tag{48}$$

Furthermore, for an interchange mode in toroidal geometry the "radial" component of the normalized displacement vector is nearly constant along a field line; that is

$$\nabla\psi\cdot\boldsymbol{\xi}(\psi,l)\approx X(\psi)+\delta^2 X_1(\psi,l) \tag{49}$$

The next step is to recall that as $D_Q\to\infty$ the perturbations in the quasilinear region satisfy the ideal MHD equations. All transport effects can be neglected because of the fast time scale associated with quasilinear diffusion.

Under this set of assumptions it is straightforward to show, in analogy with Eq. (13), that the magnetic field can be expressed in terms of a flux function. This equation, when rewritten in flux coordinates, yields an expression for the relative motion of the background fluid velocity with respect to the background flux coordinate.

$$v_\psi + \frac{1}{RB}\frac{\partial \psi}{\partial t} = -\frac{\tilde{v}_\psi \tilde{B}}{B} \tag{50}$$

Here the subscript "ψ" denotes normal component and $\tilde{B} = \left|\tilde{\mathbf{B}}_\parallel\right|$

The quasilinear equations describing the evolution of the background state are now obtained by averaging the density and energy equations over l and ζ, and then substituting Eq. (50), yielding

$$\begin{aligned}
\frac{\partial}{\partial \tau}(nV) &= -\frac{1}{2\pi}\int_0^{2\pi} d\zeta \oint dl \left\{\frac{\partial}{\partial \psi}\left[R\tilde{v}_\psi\left(\tilde{n} - \frac{n}{B}\tilde{B}\right)\right]\right\} \\
\frac{\partial}{\partial \tau}(sV) &= -\frac{1}{2\pi}\int_0^{2\pi} d\zeta \oint dl \left\{\frac{\partial}{\partial \psi}\left[R\tilde{v}_\psi\left(\tilde{s} - \frac{s}{B}\tilde{B}\right)\right]\right\}
\end{aligned} \tag{51}$$

The final step in the analysis is to eliminate $\tilde{v}_\psi, \tilde{n},$ and $\tilde{s}$ using the linearized equations of ideal MHD stability. Only the conservation of mass and energy relations are required. Consistent with the assumptions made above we find that

$$\begin{aligned}
\tilde{v}_\psi &\approx \frac{1}{RB}\frac{\partial X}{\partial \tau} = \frac{1}{RB}\sum_n \gamma_n X_n(\psi)\exp(\gamma_n \tau + in\zeta) \\
\tilde{n} &\approx -X\frac{\partial n}{\partial \psi} - n\nabla\cdot\boldsymbol{\xi}_\perp \\
\tilde{s} &\approx -X\frac{\partial s}{\partial \psi} - s\nabla\cdot\boldsymbol{\xi}_\perp
\end{aligned} \tag{52}$$

The quasilinear evolution equations reduce to

$$\begin{aligned}
\frac{\partial}{\partial \tau}(nV) &= \frac{\partial}{\partial \psi}\left[\bar{D}_Q \frac{\partial}{\partial \psi}(nV)\right] \\
\frac{\partial}{\partial \tau}(sV) &= \frac{\partial}{\partial \psi}\left[\bar{D}_Q \frac{\partial}{\partial \psi}(sV)\right]
\end{aligned} \tag{53}$$

where

$$\bar{D}_Q = \sum_n \gamma_n |X_n|^2 \tag{54}$$

These are the desired equations. Note that as in the cylindrical case no use has been made of the linearized momentum equation.

- **Final form of the toroidal quasilinear transport equations**

The formulation of the steady state quasilinear transport equations can now be easily obtained by setting $\partial / \partial \tau = 0$ and specifying boundary and jump conditions as outlined in the cylindrical model problem. The results are as follows.

Classical region:

$$\begin{aligned} &\frac{\partial}{\partial \psi}\left(\bar{D}_C T^{3/4} \frac{\partial n T^{1/4}}{\partial \psi} \right) = 0 \qquad && \frac{\partial n(\psi_c)}{\partial \psi} = 0 \\ &\frac{\partial}{\partial \psi}\left(n \bar{\chi}_C \frac{\partial T}{\partial \psi} \right) + \langle S \rangle V = 0 \qquad && T(\psi_c) = 0 \end{aligned} \tag{55}$$

Quasilinear region:

$$\begin{aligned} &\frac{\partial nV}{\partial \psi} = 0 \qquad && n(\psi_w) = n_w \\ &\frac{\partial sV}{\partial \psi} = \frac{1}{(nV)^{\gamma-1}} \frac{\partial p V^{\gamma}}{\partial \psi} = 0 \qquad && s(\psi_w) = p_w / n_w^{\gamma-1} \end{aligned} \tag{56}$$

Jump conditions:

$$\begin{aligned} [\![n]\!]_{\psi_s} &= 0 \\ [\![p]\!]_{\psi_s} &= 0 \end{aligned} \tag{57}$$

Definition of ψ_s:

$$\left.\frac{\partial pV^{\gamma}}{\partial \psi}\right|_{\psi_s^-} = 0 \tag{58}$$

As in the cylindrical case the quasilinear energy equation coincides with the marginal stability criterion for interchange modes: $\partial pV^{\gamma}/\partial\psi \geq 0$.

Lastly, note that the equations in the quasilinear region can be rewritten in forms more closely analogous to the cylindrical results. A short calculation yields

$$\begin{aligned} -\frac{1}{\langle \kappa / RB \rangle}\left(\frac{1}{n}\frac{\partial n}{\partial \psi}\right) + \frac{2}{1+\mu_0 \gamma p \langle 1/B^2 \rangle} = 0 \\ -\frac{1}{\langle \kappa / RB \rangle}\left(\frac{1}{p}\frac{\partial p}{\partial \psi}\right) + \frac{2\gamma}{1+\mu_0 \gamma p \langle 1/B^2 \rangle} = 0 \end{aligned} \tag{59}$$

where $\kappa = \mathbf{n}\cdot(\mathbf{b}\cdot\nabla\mathbf{b}) < 0$ is the normal component of the curvature.

The quasilinear toroidal dipole problem is now fully specified. When solved it leads to a prediction of both the steady state pressure and density profiles from which it is then straightforward to calculate macroscopic quantities of interest such as β and τ_E.

VI. Numerical simulations

We next attempt to verify the conclusions of the quasilinear transport model by means of a nonlinear simulation. To understand the numerical simulations recall that the validity of the quasilinear transport model requires that several assumptions be satisfied. These assumptions can be quantified in terms of four characteristic time scales that appear in the problem. The longest time scale $\tau_C \simeq a^2/\chi_C$ corresponds to classical heat diffusion. Next in the hierarchy is the heating time $\tau_H \simeq p/S$. The assumption is that the plasma is heating up faster than it can lose energy by classical heat conduction. The third time scale $\tau_Q \simeq a^2 / D_Q$ is the quasilinear diffusion time. By definition quasilinear diffusion should dominate energy transport, preventing the plasma from reaching the high temperatures that would result from purely classical transport. The fastest time scale $\tau_M \simeq a / v_{Ti}$ corresponds to the characteristic growth rate of MHD instabilities and enters into the expression for D_Q. Thus, for quasilinear theory to be valid we require that

$$\tau_M \ll \tau_Q \ll \tau_H \ll \tau_C \tag{60}$$

An equivalent interpretation in terms of perturbation amplitudes is as follows. The amplitudes of the MHD perturbations and the corresponding growth rates should be large enough so that quasilinear diffusion dominates the particle and energy transport but must be small enough so that the non-linear terms are unimportant.

The numerical simulations described in this Section have two primary objectives: (1) demonstrate that in appropriate parameter regimes of experimental interest the quasilinear model accurately predicts plasma transport, and (2) determine the time evolution of the profiles and demonstrate the existence of the self-consistent steady state plasma profiles predicted by the quasilinear model. A key additional point is to assess the validity and accuracy of the numerical codes used for the simulations. This last point, as we shall see, is problematic because of the highly localized structure of the interchange eigenfunctions. Because of this the simulation results are only partially satisfactory in achieving our objectives.

- **The numerical model**

The code used to simulate the evolution of the plasma is a modified version of the earlier one-fluid code developed at University of Maryland [15]. The code solves the following system of equations

$$\begin{aligned}
&\text{Mass:} && \frac{\partial\rho}{\partial t}+\nabla\cdot(\rho\mathbf{v})=0\\
&\text{Ohm's law:} && \frac{\partial\mathbf{B}}{\partial \mathrm{t}}=\nabla\times\left(\mathbf{v}\times\mathbf{B}\right)+\eta\nabla^2\mathbf{B}\\
&\text{Momentum:} && \rho\left(\frac{\partial\mathbf{v}}{\partial t}+\mathbf{v}\cdot\nabla\mathbf{v}\right)=\mathbf{J}\times\mathbf{B}-\nabla p-\nabla\cdot\left(\mu\rho\nabla\mathbf{v}\right)\\
&\text{Energy:} && \frac{d}{dt}\left(\frac{p}{\rho^\gamma}\right)=\frac{2}{3\rho^\gamma}\left[S_E+\nabla\cdot\left(\rho\chi_\perp\nabla_\perp T+\rho\chi_\parallel\nabla_\parallel T\right)\right]
\end{aligned} \tag{30}$$

The geometry corresponds to a 2-D cylindrical hard core Z-pinch. The parameters μ , η , $\chi_\perp$ and $\chi_\parallel$ are viscosity, resistivity, cross-field and parallel classical conduction coefficients respectively, with $\chi_\parallel \gg \chi_\perp$. Each of these coefficients is held constant during the simulation. As is characteristic of virtually all MHD fluid codes the transport coefficients are substantially larger than their actual physical values in order to insure good numerical convergence. This convergence requirement, we shall see, is the main feature that makes the interpretation of the numerical results problematic.

In the simulations the plasma is confined in a perfectly conducting cylindrical shell of radius $r_w = 1.1\ m$. The plasma is stabilized by an inner coil (i.e. the hard core) carrying a 10 kA current. The coil radius is $r_c = 0.1\ m$.

All functions are assumed to be periodic in the *z*-direction (i.e axial) with the length of the box $L = 3.0\ m$. Typical simulations were carried out with a grid resolution of $r \times z = 100 \times 300$. The temperature boundary conditions on the wall and coil walls assume that these surfaces are maintained at a constant temperature $T_c = T_w = 0.1\ eV$. The number of particles in the simulated volume is held fixed, so the plasma neither looses nor gains any additional mass. Finally, the energy source is modeled by a relatively broad Gaussian function $S_E \propto \exp\left[-\left(r-r_h\right)^2/2\Delta r^2\right]$ located $20\ cm$ away from the coil: $r_h = 30\ cm$ and $\Delta r \approx 7\ cm$.

- **Weak heating simulation**

The starting point for the simulations corresponds to a cold plasma with a flat density profile and the background temperature equal to the wall temperature $T\left(t=0\right)=T_w$. The first numerical experiment involves a low-energy heating source (i.e. S is small) that slowly heats the plasma to a level that is just slightly unstable against interchange modes. The z-averaged density and pressure profiles for the barely overheated plasma are illustrated in Fig. 3. Observe that the particle density is lowered in the plasma core due to both the frozen-in law, which carries particles within the magnetic flux tubes and slow collisional transport; that is, the finite resistivity creates a slow collisional particle flux, which drives particles into the regions of low temperature $\Gamma^p \propto -D_c \partial\left(nT\right)/\partial r$.

The stability condition is first violated close to the outer wall causing the plasma to develop a small-scale convective motion as illustrated on Fig. 4. The amplitudes of the perturbations are quite small implying that quasilinear diffusion should dominate nonlinear effects. However, the growth rates of the modes are also quite small, implying that the quasilinear diffusion coefficient is small. In other words the additional quasilinear transport does not dominate classical conduction (for the numerical values used in the simulations) and therefore does not noticeably change the plasma profiles.

The conclusion is that when S is too small quasilinear transport occurs but is too weak to dominate over classical transport.

- **Strong heating simulation**

The second set of numerical experiments involves a stronger external heating source (i.e. S is large), which deposits 10 times the maximum energy allowed by classical heat conduction that would not violate the MHD stability criterion. As the instabilities develop, the plasma undergoes a macroscopic transformation, leading to the formation of fast moving convective cells. Such behavior can be analyzed only in a non-linear model. The interchange instabilities and corresponding non-linear transport dominate over collisional transport (i.e. only about 10% of the energy flux is due to collisional transport) and leads to an equilibration of the number of particles on any given flux tube. Several different snapshots in the evolution of the particle density are illustrated in Fig. 5.

The eventual density profile is close to $\rho \sim 1/V \sim \left(\oint dl/B\right)^{-1}$ in the MHD unstable region, though it never reaches the exact "target" profile given by Eq. (37) due to the presence of collisional transport. The density profile in the MHD stable region is also seen to undergo significant changes on a fast time scale due to the small volume of the region and the strong velocity changes in the convective cells, which bring particles in or out of the inner region of plasma. A comparison of density and pressure profiles at the time $t = t_4$ and the "target" profiles is illustrated in Fig. 6.

The pressure profile evolves to its marginally stable form in the outer region, governed by Eq. (37) except in a narrow boundary layer at the outer wall, where viscosity plays an important role. This type of self-organization and redistribution of plasma profiles towards the marginally stable ones has also been reported by V.Makhnin *et.al*. [11].

The major mechanism of energy transfer in the present simulations is the large-scale convective cell motion of the plasma, as seen in Fig.7. This behavior coincides with that seen by Pastukhov [9] in the quasi-stable state, while Makhnin reported smaller scale incoherent turbulence. Also, the development of large-scale convective cells in the non-linear regime is supported by the theoretical analysis presented by Yoshizawa *et.al*.[16].

The existence of the global convective cells protects the plasma against disruptions by providing a mechanism to disperse the excessive heat from the plasma core. At the same time, during the formation of the convective cells and reorganization of the plasma profiles, a large radial velocity is observed only a few grid points away from the outer wall. That suggests that the rapid overheating of the plasma and the creation of strong non-linear perturbations may lead to large energy transport into the wall if a less ideal and more realistic boundary condition were used in the simulations.

- **Summary of simulation results**

Quasilinear transport has not been seen to play the dominant role in energy transport in the present numerical studies. It was observable for the case of a weak energy source, but its magnitude was not large enough to dominate classical transport. For the high power heat source, quasilinear transport was present and large but was quickly replaced by the non-linear stage. A similar finding was reported by Pastukhov [9]. He observed that the quasilinear transport started to smooth the profiles, but was not dominant and was replaced by non-linear global plasma motion. The conclusion is that we do not have clear numerical evidence that demonstrates a regime where quasilinear energy and particle diffusion are the dominant transport mechanisms although, interestingly, the nonlinear results yield the same steady state profiles. However, as discussed below, the difficulties may well be due to the limitations of the simulations rather than the quasilinear theory

Specifically, the absence of quasilinear dominated transport may simply point out the difficulties of the numerical codes to describe fine scale perturbation, even if their theoretical growth rates are large. One factor is that the numerical grid restricts the entire spectra of the unstable perturbations to only the longer scale perturbations with the minimum allowable wavelength equal to 5-7 grid points. This reduces the quasilinear diffusion coefficient to only a few slower growing modes, thereby invalidating some of the assumptions for the validity of the theory. A finer resolution may partially improve the situation by including shorter wavelength modes, but even this may not be sufficient to capture the true micro-structure of the modes, which may well make the largest contribution to quasilinear transport.

A second numerical problem is that in order to keep the run time reasonably short, the initial conditions and heating source amplitude are chosen so that when instabilities are excited, they have significant amplitudes, which are closer to the threshold of nonlinear behavior than might be expected by the slower, weak amplitude evolution required by quasilinear theory. In other words the larger mode amplitudes required by the simulations essentially preclude, by definition, the possibility of a weak amplitude quasilinear evolution.

Thus, while both the nonlinear and quasilinear results lead to the same final profiles it is not yet clear which model most closely models the actual experimental situation. This remains an area of future research.

VII. Conclusions

It has been analytically shown that the excitation of interchange modes leads to a quasilinear transport of both energy and particles transport. The quasilinear transport is independent of collisional mechanisms. Its major contribution comes from the mixing of short wavelength perturbations. This micro turbulence transport effectively restores pressure profile to its marginally stable form and causes the density profile to evolve to $\rho \sim \left[\int dl/B\right]^{-1}$.

The exact transport equations are derived for a hard core Z-pinch magnetic configuration. The transport equations are generalized to an axisymmetric closed-field line toroidal geometry under the assumption of including only short-wavelength perturbations.

The quasilinear transport analysis has been derived under the assumption of weakly unstable plasma profiles. To test the applicability of initial assumption, a set of nonlinear numerical simulations has been carried out. The simulations were unable to show that the quasilinear transport can be sufficiently dominant to significantly change plasma profiles. Instead, the major transport mechanism observed in the strongly unstable case was nonlinear global convective cells. The convection reorganized the pressure and density profile to the same steady-state profiles predicted by quasilinear theory, although the mechanisms were different. This somewhat unsatisfactory result may well be explained by the natural limitations of the numerical codes, which involve grid resolution and incompatible initial conditions.

In any event, the overlap of the results allows us to make a prediction for the steady state β and τ_E for LDX, two parameters of experimental performance. This anaylsis is carried out in the accompanying paper.

Acknowledgements

The authors are extremely grateful to Sheung-wah Ng and Adil Hassam (University of Maryland) for their expertise and help with the numerical code. This research was supported by the U.S. Department of Energy grant #DE-FG02-91ER-54109 to the Plasma Science and Fusion Center at MIT

References:

1. Kesner, J., Bromberg, L., Garnier, D., Mauel, M., presented at 17th IAEA Conference of Plasma Physics and Controlled Nuclear Fusion, Yokohama, Japan 1998, paper IAEA-F1-CN-69/
2. D.T. Garnier, et al *"The Superconducting Levitated Dipole Experiment (LDX)", 15th Intl Toki Conference*, submitted to Fusion Engineering and Design.
3. D. Garnier, J. Kesner and M. Mauel, Phys. Plasmas, vol. **6**, (1999) pp.3431-3434
4. Simakov A., P. Catto, J. Ramos and R. Hastie, Phys. Plasmas, **9**, 4985 (2002).
5. Simakov A., P. Catto and R. Hastie, Phys. Plasmas, **8**, #10, p. 4414 (2001)
6. N. Krasheninnikova and P. Catto, Phys. Plasmas, **13,** 052503 (2006)
7. Glasser A. H. *et al*., Plasma Phys. Controlled Fusion, **41**, A747 (1999)
8. D.Ryutov, B.Cohen, R. Cohen, E. Hooper and C. Sovinec, Phys. Plasmas **12**, 084504 (2005)
9. V.P. Pastukhov and N.V.Chudin, Plasma Physics Reports, Vol. **27**, #11 (2001) pp. 907-921
10. V. P. Pastukhov and N. V. Chudin, 19th IAEA Fusion Energy Conf. Paper IAEA-TH/2-5, Lyon, France, 2003
11. V.Makhnin *et. al*, Phys. Plasmas **12**, 042312 (2005)
12. D. Adler and A. Hassam, Phys. Plasmas, **12**, 062506 (2005)
13. T. H. Stix, "Waves in plasmas", Springer, New-York, (1992), pp. 445-515
14. Kadomtsev B. B., in *"Reviews of Plasma Physics"*, edited by M. A. Leontovich, Consultants Bureau, New York, Vol. II. (1966)

15. P. N. Guzdar, J. F. Drake, D. McCarty, A. Hassam and C. Liu, Phys. Fluids B **5**, 3712 (1993)

16. Yoshizawa A., S. Itoh, K. Itoh and N. Yokoi, Plasma Phys. Cont. Fusion, **43** (2001), R22

Figure Captions

1. The LDX schematic profile
2. Radial pressure profiles for classical, full quasilinear and simplified quasilinear transport models.
3. The pressure and density profiles of a slowly heated plasma
4. Convective cells in a slowly heated plasma. Plasma velocity field.
5. The snapshots of the "self-organizations" process. Time t_1 - before an instability is excited; $t_2 - t_4$: different stages of self-organization
6. Comparison of (a) density and (b) pressure profiles at time t_4 with the quasilinear idealistic profiles given by Eq. (37)
7. Typical velocity field profile in a plasma.

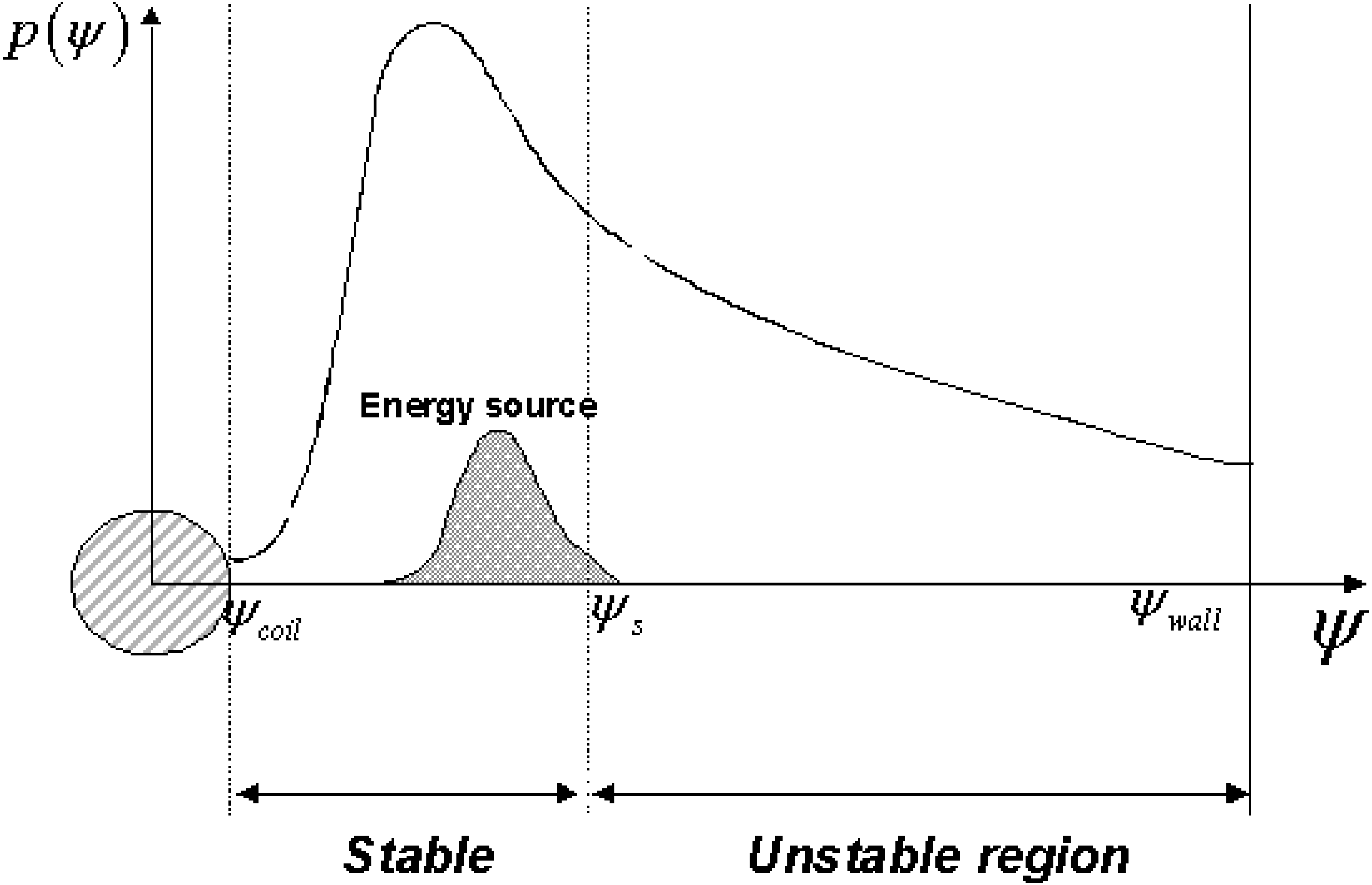

$p(\psi)$
Energy source
ψ_{coil}
ψ_s
ψ_{wall}
ψ
Stable
Unstable region

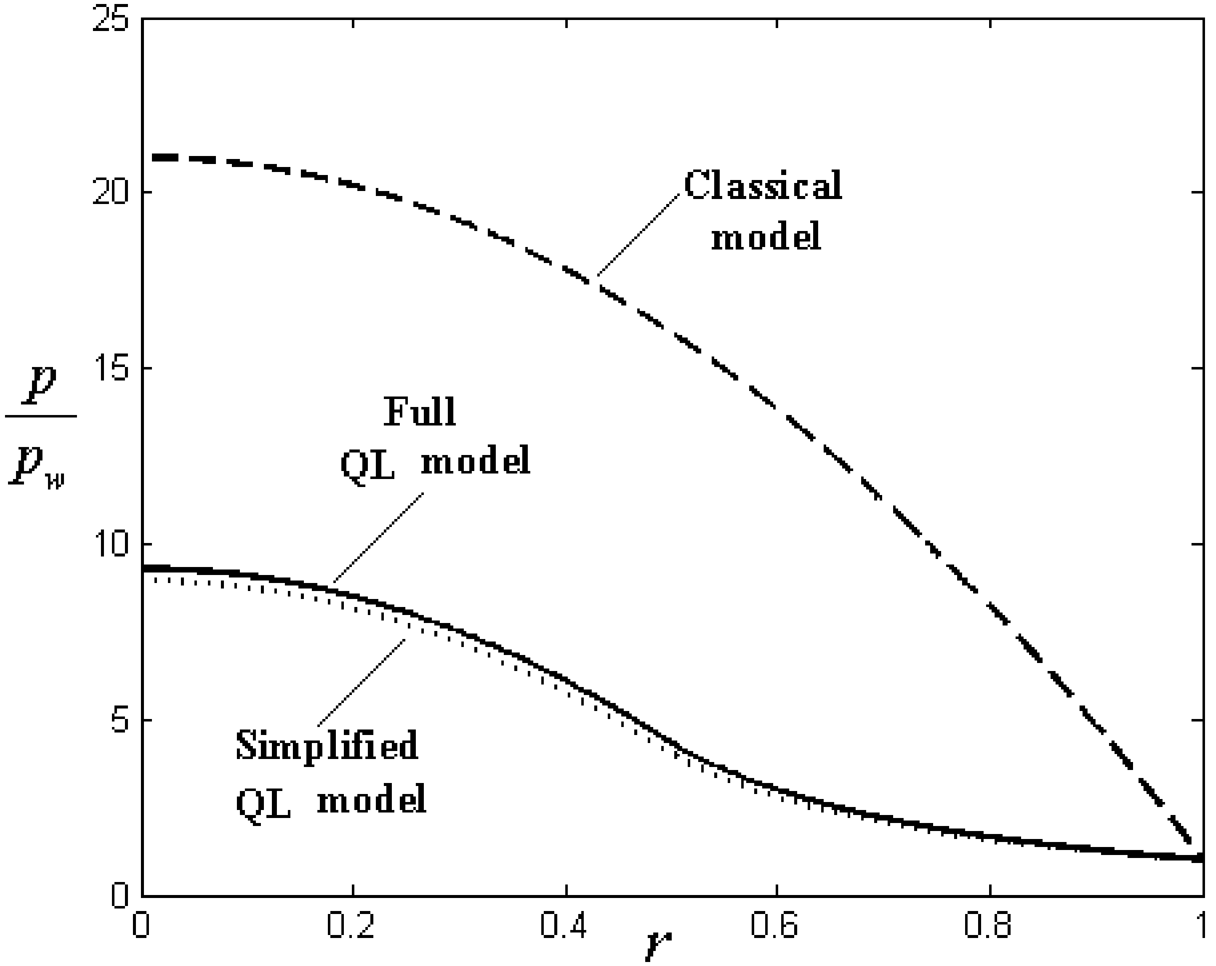

25
20
15
10
5
0
0
0.2
0.4
0.6
0.8
1
r
$\frac{p}{p_w}$
Classical model
Full QL model
Simplified QL model

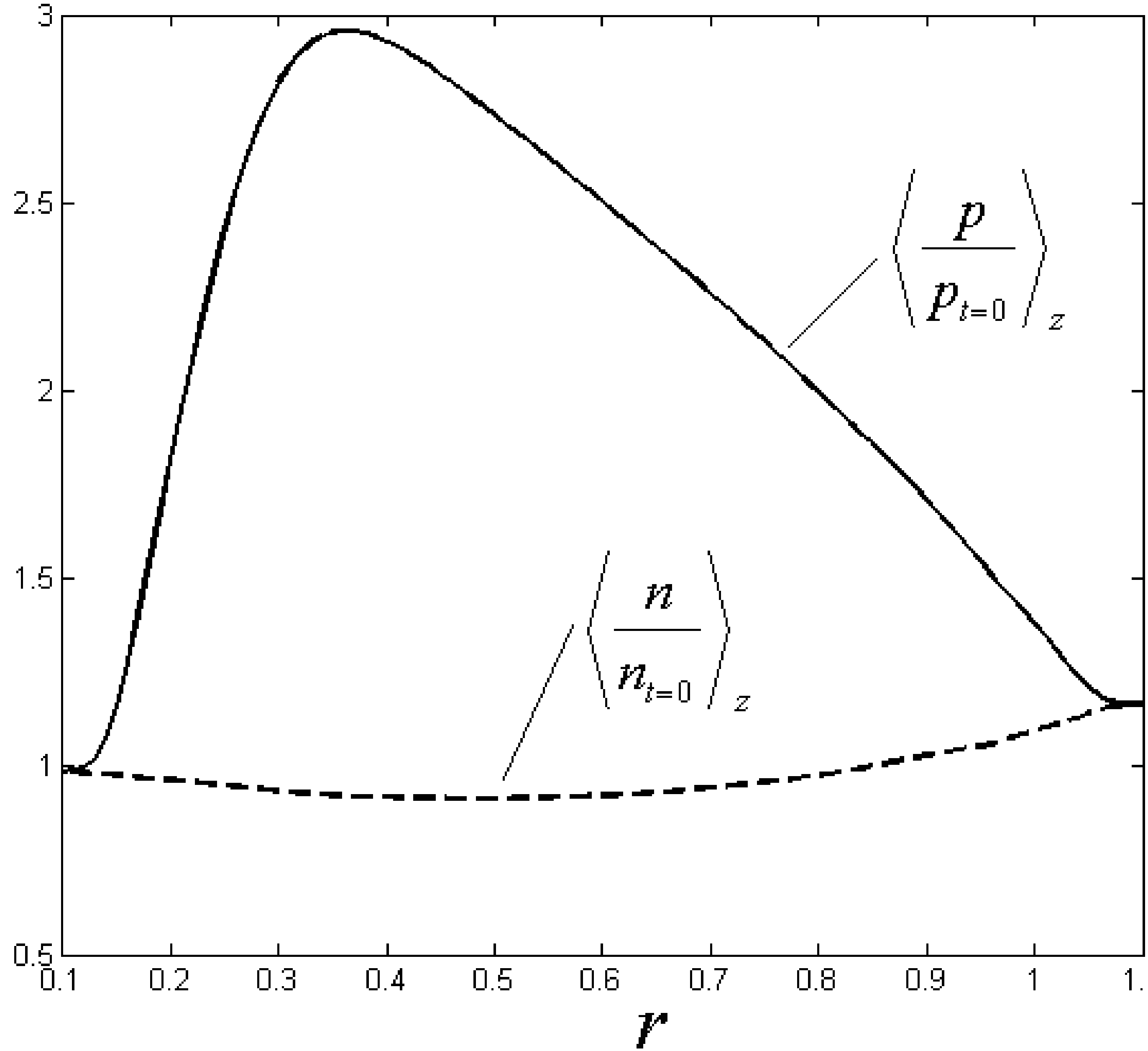

3
2.5
2
1.5
1
0.5
0.1
0.2
0.3
0.4
0.5
0.6
0.7
0.8
0.9
1
1.1
r
$\left\langle \frac{p}{p_{t=0}} \right\rangle_z$
$\left\langle \frac{n}{n_{t=0}} \right\rangle_z$

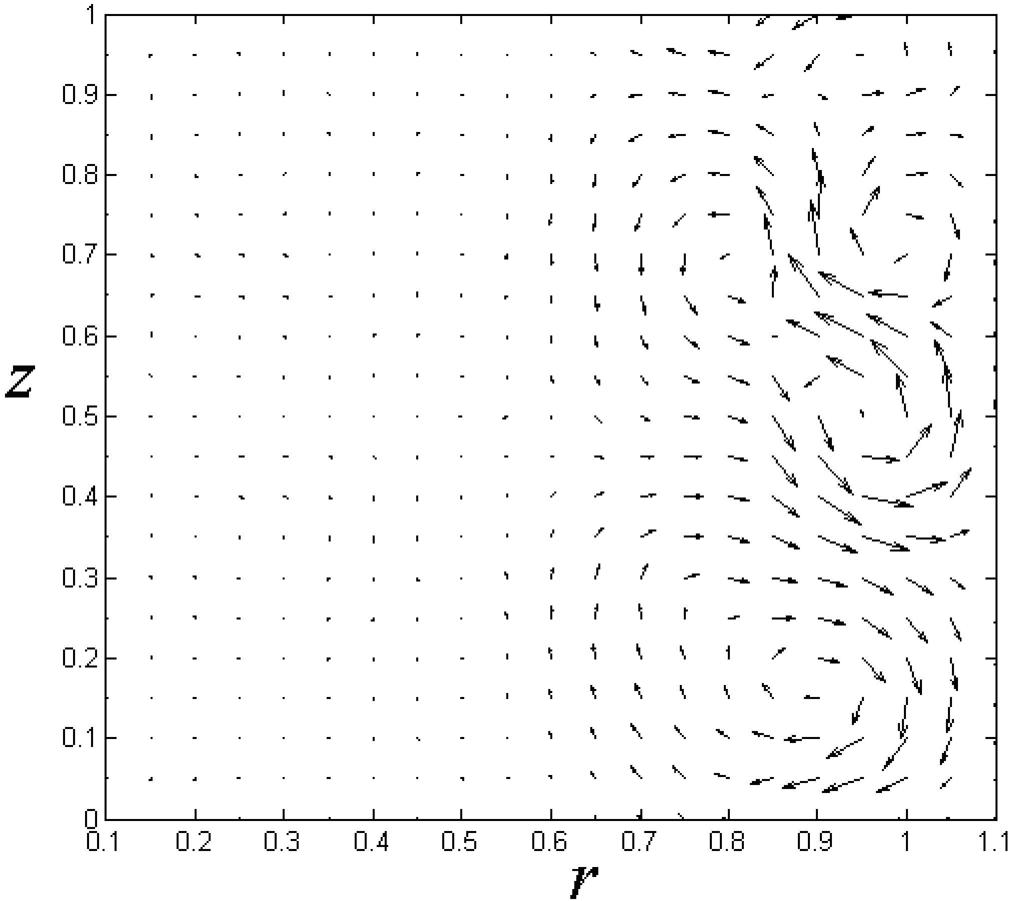

z
r
0
0.1
0.2
0.3
0.4
0.5
0.6
0.7
0.8
0.9
1
1.1

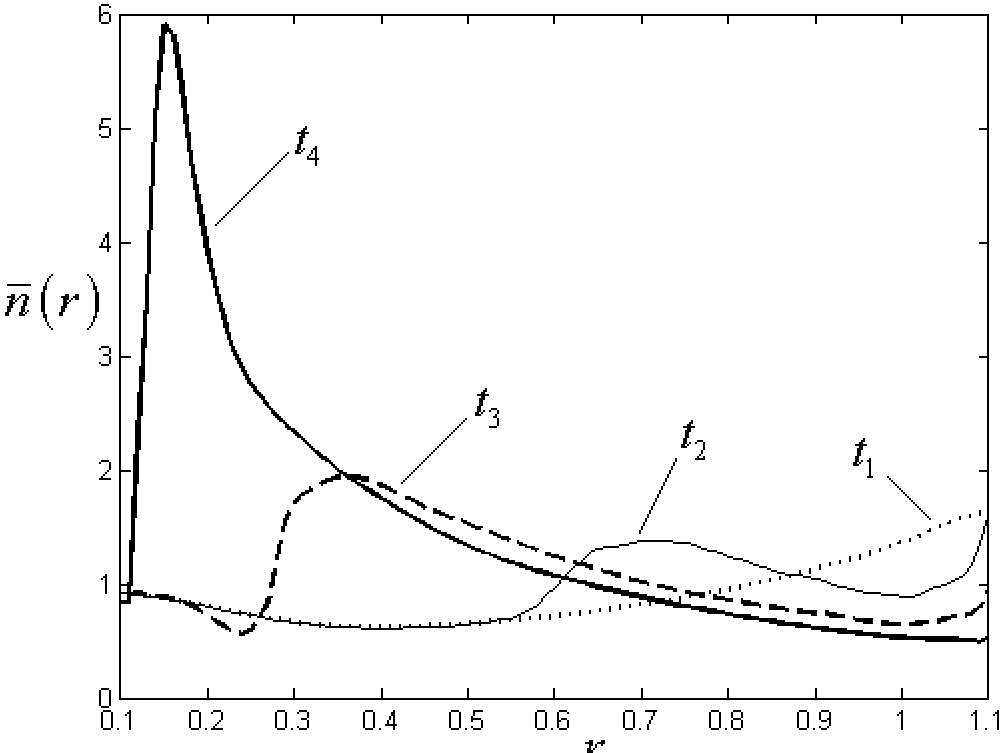

$\overline{n}(r)$
r
t_4
t_3
t_2
t_1
0
1
2
3
4
5
6
0.1
0.2
0.3
0.4
0.5
0.6
0.7
0.8
0.9
1
1.1

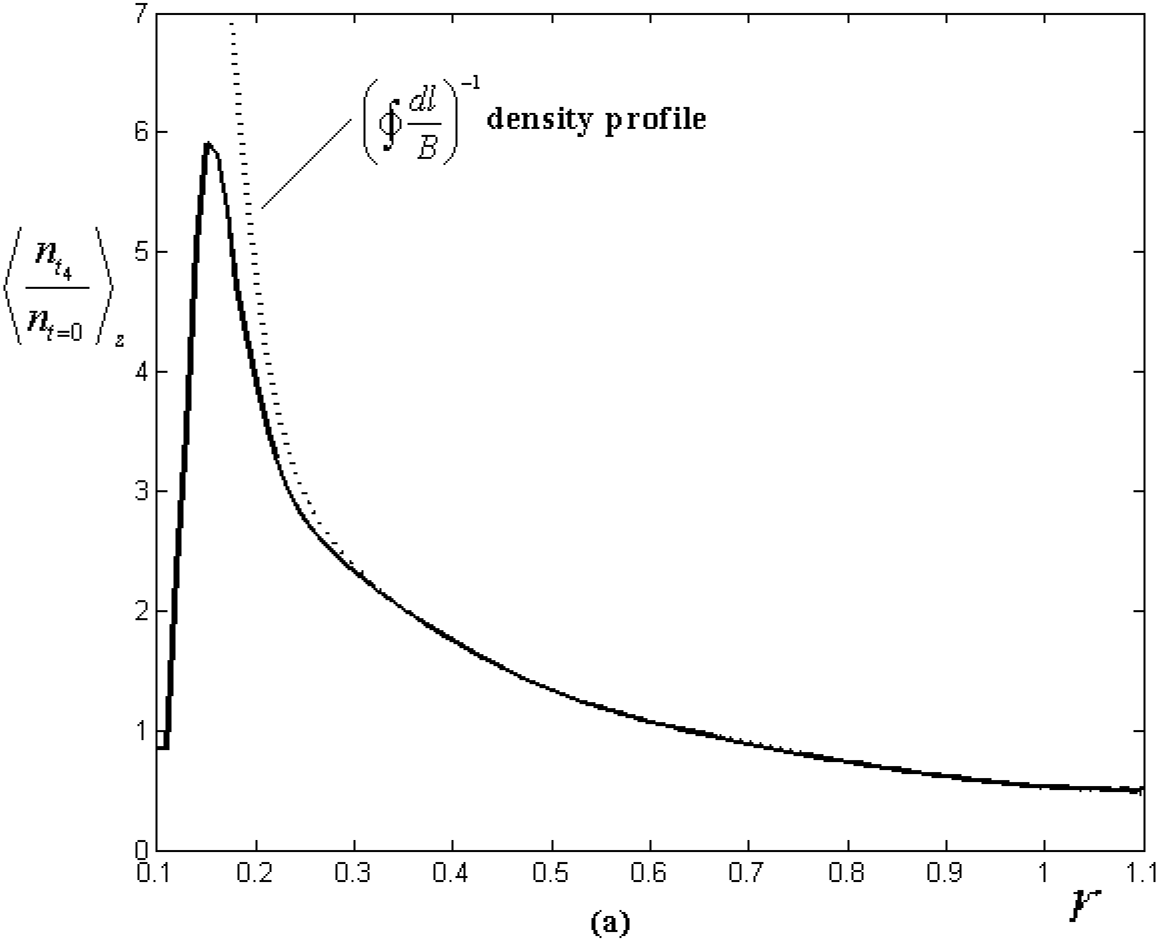

7
6
5
4
3
2
1
0
0.1
0.2
0.3
0.4
0.5
0.6
0.7
0.8
0.9
1
1.1
$\left\langle \frac{n_{t_4}}{n_{t=0}} \right\rangle_z$
r
$\left(\oint \frac{dl}{B}\right)^{-1}$ density profile

(a)

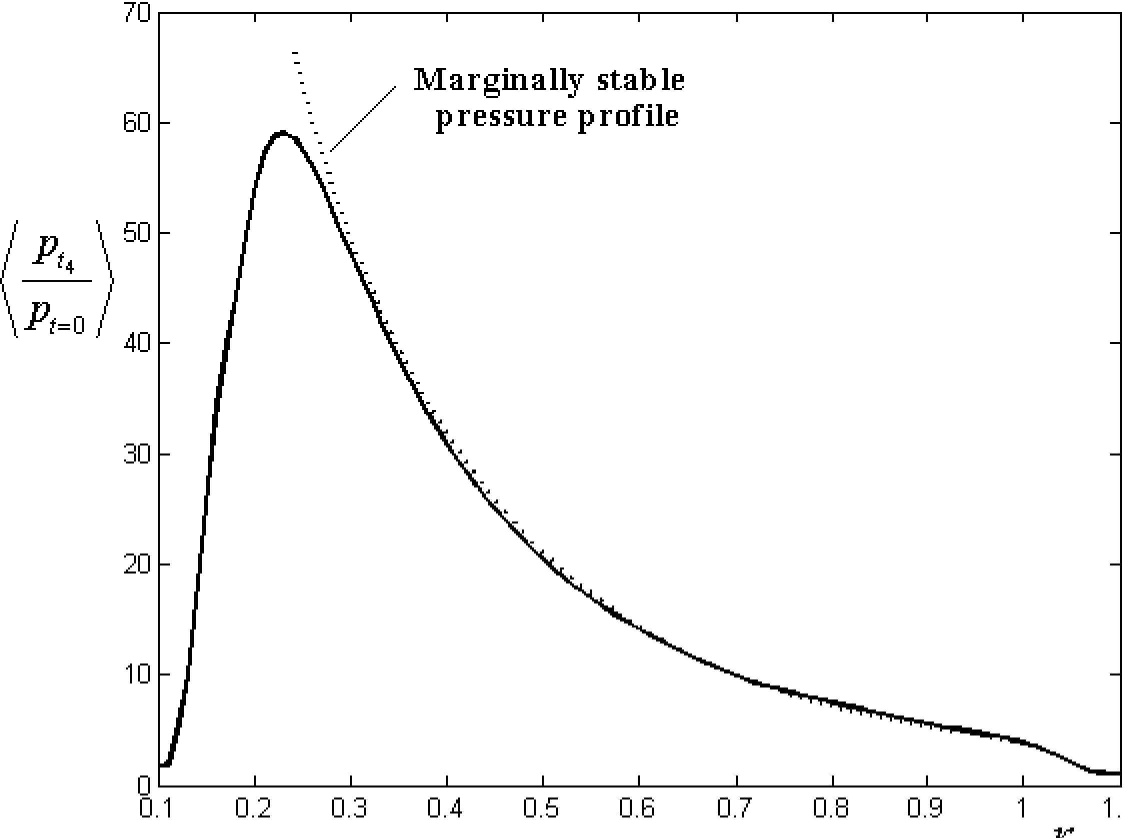

Marginally stable
pressure profile
$\left\langle \frac{p_{t_4}}{p_{t=0}} \right\rangle$
r
0
10
20
30
40
50
60
70
0.1
0.2
0.3
0.4
0.5
0.6
0.7
0.8
0.9
1
1.1

(b)

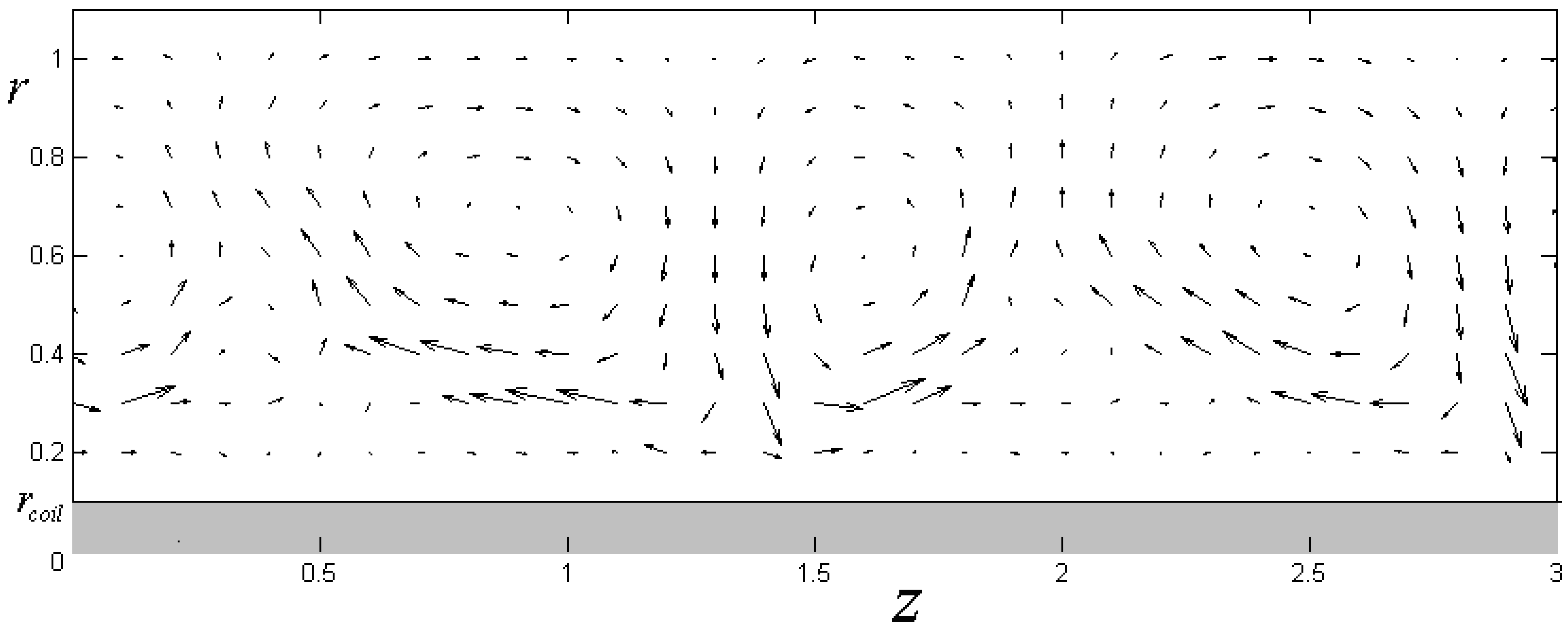

r
1
0.8
0.6
0.4
0.2
r_{coil}
0
0.5
1
1.5
2
2.5
3
z